International Journal of Precision Engineering and Manufacturing-Green Technology (2021) 8:501–508
https://doi.org/10.1007/s40684-020-00205-7

Online ISSN 2198-0810
Print ISSN 2288-6206

REGULAR PAPER

Optical and Electrical Properties of Multilayer Grid Electrodes for Highly Durable Transparent Conductive Electrodes

Hyo-Ju Lee[1] · Ki-Yeop Cho[1] · Semi Oh[2] · So-Yeon Park[3] · Ye-Bin Im[3] · Suyeon Son[3] · Yong-Jin Yoon[4] · Seong-Ju Park[1] · Kyoung-Kook Kim[3]

Received: 11 November 2019 / Revised: 10 February 2020 / Accepted: 17 February 2020 / Published online: 27 March 2020

Abstract

We report on the optical and electrical properties of MgZnO/Ag/MgZnO (MAM) grid electrodes grown at room temperature; these are proposed as an alternative to metal-based grid electrodes to meet the requirement for high stability in a harsh environment. The optical transmittance of Ag grid electrodes improved when the Ag grid layer was embedded in an MgZnO grid layer regardless of the fill factor. This improvement depends critically on the Ag grid layer thickness in the MAM grid electrodes. The Haack figure of merit for a MAM grid electrode with a 20 nm-thick Ag grid layer was approximately threefold higher than that of an Ag grid electrode. The electrode has an average transmittance of 85.8% at wavelengths range from 400 to 1100 nm and a sheet resistance of 26.9 Ω/sq. These results indicate that MAM grid electrodes can be an alternative to metal-based grid electrodes in optoelectronic devices that require stable wideband operation in a harsh environment and over a wide wavelength region.

Keywords MgZnO/Ag/MgZnO · Grid electrodes · Transparent conductive electrodes · High stability · IR transmittance

Nomenclature

R	Sheet resistance
G	Spacing size between grid lines
W	Width of grid metal lines
T	Transmittance
τ	Correction factor

1 Introduction

Transparent conductive electrodes (TCEs) are one of the key components in many optical and electrical devices, including photovoltaic cells, light-emitting diodes, and touch screen panels. Indium tin oxide (ITO), one of the typical TCEs, has been widely used for TCEs in many optical and electrical devices [1–3]. However, the ITO has the drawbacks of low flexibility, high cost, and high-temperature processing.

Metal-based electrodes such as metal nanowires and metal grids have attracted attention as a possible alternative to ITO because they exhibit high electrical and optical properties as well as superior flexibility [4–11]. Even though metal-based electrodes have very useful characteristics, the Ag and Cu used in these electrodes have poor adhesion to substrates and low thermal and chemical stability [12, 13].

Recently, dielectric/metal/dielectric (DMD) multilayer films such as ITO/Ag/ITO, MgZnO/Ag/MgZnO (MAM), ZnO/Ag/ZnO, MoO_3/Ag/MoO_3, and TiO_2/Ag/ZnO have been investigated by many research groups utilizing these films' high electrical conductivity and optical transparency at visible wavelengths [14–21]. However, film-based DMD multilayer electrodes have limited application to optical devices that require transparency in broad wavelength regions because their films usually have low transparency

Hyo-Ju Lee and Ki-Yeop Cho contributed equally to this work.

✉ Kyoung-Kook Kim
kim.kk@kpu.ac.kr

[1] School of Materials Science and Engineering, Gwangju Institute of Science and Technology, 123 Cheomdangwagi-ro, Buk-gu, Gwangju 61005, Republic of Korea

[2] Department of Electrical Engineering and Computer Science, University of Michigan, 1301 Beal Avenue, Ann Arbor, MI 48109, USA

[3] Department of Nano Optical Engineering, Korea Polytechnic University, 237 Sangidaehak-ro, Siheung-si, Gyeonggi-do 15073, Republic of Korea

[4] Department of Mechanical Engineering, Korea Advanced Institute of Science and Technology, 291 Daehak-ro, Yuseong-gu, Daejeon 34141, Republic of Korea

in the infrared (IR) region due to free-electron reflectance in the metal layer.

Also, Choi et al. reported highly durable AgNi grid electrodes, which exhibit high stability against oxidation and high temperature as well as strong adhesion to substrates when compared with Ag grid electrodes [20]. However, the sheet resistance of AgNi is higher than that of Ag grid electrodes because of the intrinsic low conductivity of AgNi, compared with that of pure Ag.

Here, we propose a MAM grid electrode design and report that these high-performance and high-durability multilayer grid electrodes can meet the requirements of TCE applications. Although the thickness of Ag in a multilayer grid electrode is thinner than Ag grid electrodes, multilayer grid electrodes show better electrical and optical properties in the IR wavelength range than film-based DMD structures and also exhibit higher durability in a harsh environment than Ag grid electrodes. This makes the multilayer grid electrode a viable alternative to the conventional ITO electrode or metal-based grid electrode in environmentally rugged devices.

2 Experimental

Glass substrates were successively cleaned in acetone, methanol, deionized water and isopropyl alcohol in an ultrasonic bath for 15 min and then were dried in an oven. After the cleaning process, positive photoresist was spin-coated and patterned on the substrates with a standard photolithography technique. A 50 nm-thick MgZnO bottom layer was deposited on a patterned substrate at room temperature (RT) with radio-frequency (RF) magnetron sputtering using two targets: one consisting of pure ZnO, the other of ZnO mixed with MgO (20 wt%). The surface of the patterned MgZnO bottom layer was pretreated with Ar ions from a gridless end-Hall ion source to improve the Ag layer's wetting property on the dielectric substrate. The ion beam treatment process conditions were equivalent to those previously reported in our journal [18]. The Ag grid layer was then deposited on the patterned MgZnO bottom layer with electron beam evaporation. Next, the overcoat MgZnO (50 nm) layer was deposited on the Ag thin film with RF magnetron sputtering. Finally, the multilayer grid structure was dipped into acetone and placed in an ultrasonic bath until the photoresist was completely lifted off. The optical and electrical properties of the gird electrodes were critically depend on the adhesion of Ag layer on the substrate because the ultra thin Ag layer is easily peeled off on the substrate during the lift-off process. To improve the reliability of sheet resistance values and optical transmittance, we processed ion beam pretreatment after deposition of MgZnO bottom layer. The specular transmittance of the multilayer grids was characterized using a UV–VIS spectrometer (Agilent 8453) with a blank substrate as the reference in the spectral range from 400 to 1100 nm. The sheet resistance was measured by the four-point probe method (FPP-40 K, DASOL ENG) with the limited measurement range (0.4 Ω/sq ~ 40 kΩ/sq within an accuracy of ± 1%). The sheet resistance and optical transmittance were average for each samples which was measured three times. The thermal stability of multilayer grid electrodes was indicated by the change of sheet resistance from RT to 350 °C after annealing for 1 h. The oxidation resistance of multilayer grid electrodes was measured by the change of their sheet resistance of with exposure to UV-ozone. The surface of MAM grid electrodes was examined with field emission scanning electron microscopy (FE-SEM, Hitachi S-4700).

3 Results and Discussion

Figure 1a shows the transmittance of film-based Ag and MAM electrodes with various Ag thicknesses. The transmittance of MAM electrode with a 20 nm-thick Ag film was around 80% while the transmittance of an Ag (20 nm) electrode alone was only 50% because the reflectance at the surface of the metal layer was reduced by surface plasmon and antireflection effects [22, 23]. However, the improvement in transmittance was reduced with increasing Ag film thickness because the light intensity passing through the metal film was exponentially attenuated by absorption of free electron gas in the metal. In our results, the difference in transmittance between 75 nm-thick MAM and 75 nm-thick Ag electrode was only 3% as shown in Fig. 1a.

The sheet resistance of film-based Ag and MAM electrodes with various Ag thicknesses is shown in Fig. 1b. Although the sheet resistance of MAM electrodes was higher than that of Ag electrodes for thickness less than 50 nm, the sheet resistance of two electrode types was almost the same when the Ag films were thicker than 50 nm. The sheet resistance of MAM electrodes can be expressed using the following equation:

$$\frac{1}{R_{\mathrm{s}}} = \frac{1}{R_{\mathrm{Ag}}} + \frac{1}{R_{\mathrm{MgZnO}}}$$

where R_s, R_{Ag}, and R_{MgZnO} are the sheet resistance of MAM electrode, Ag electrode, and MgZnO film layer, respectively. The sheet resistance of MAM electrode was critically dependent on the Ag layer because the sheet resistance of the MgZnO layer is much higher than that of the Ag layer [24, 25]. The electrical conductivity of the MAM electrode was observed to be similar to that of the pure Ag layer for a sufficiently thick the Ag layer, as shown in Fig. 1b. Although the MAM and Ag film structures show a very low sheet resistance of less than 3Ω/sq when the Ag thickness is between 10 to 80 nm, the transmittance of these structures is still too low for a TCE application that requires more than 90%

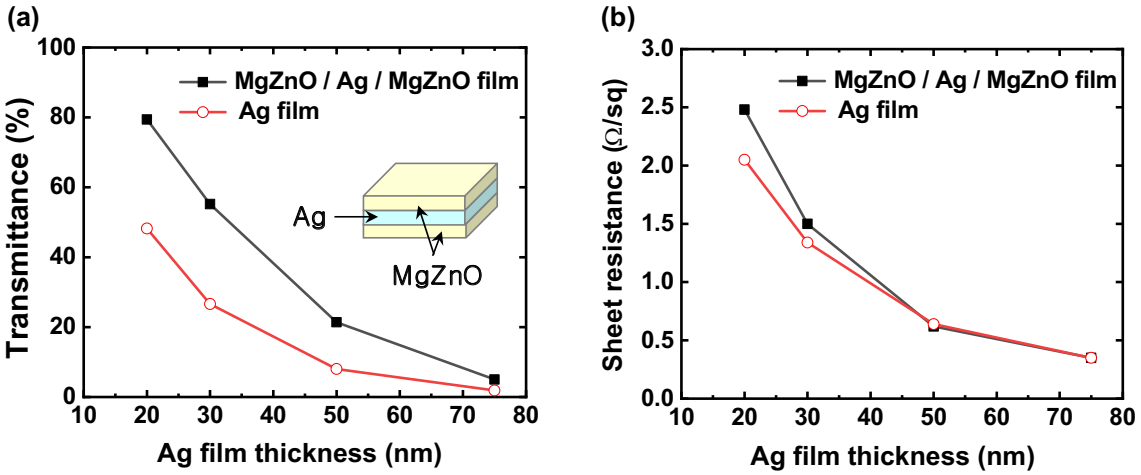

Fig. 1 **a** The optical transmittance at 550 nm and **b** the sheet resistance of film-based MAM electrodes and Ag electrodes as a function of Ag layer thickness

transmittance. In order to solve this problem in this study, we propose a MAM electrode in which both the dielectric and the metal have a grid structure.

The optical and electrical properties of metal-based grid electrodes depend on the area of metal lines on their substrates; this property is defined by the fill factor (FF), per the following equation [24]:

$$\text{Fill factor (FF)} = 1 - \frac{G^2}{(G+W)^2}$$

where G is the spacing between metal grid lines and W is the width of the lines. According to previous studies, the optical transmittance and sheet resistance of metal grid electrodes can be easily predicted from their calculated FFs [26]. The transmittance of metal grid electrodes was calculated by assuming that the metal grid lines totally blocked the transmission of light due to their high reflectance for a sufficiently thick (near 100 nm) grid. In this study, however, we calculated the FF of MAM grid electrodes by modifying the previously reported equation; because the MAM grid lines allowed light transmission. We calculated the transmittance of MAM grid electrodes using the following equation:

$$T_{total} = FF_{air} + T_{MAM}FF_{MAM}$$

where the T_{total} is total transmittance of MAM grid electrodes, FF_{air} is open area ($= 1 - FF_{MAM}$), T_{MAM} is the transmittance of the MAM grid lines, and FF_{MAM} is the FF of the MAM grid lines.

The sheet resistance of MAM grid electrodes can then be calculated by the following equation:

$$R_{s,total} = R_{s,MAM}\frac{1}{FF_{MAM}}\tau$$

where the $R_{s,total}$ is the total sheet resistance of MAM grid electrodes, $R_{s,MAM}$ is the sheet resistance of the MAM lines, and τ is a correction factor that depends on the process conditions and grid structure [26].

Figure 2a shows the schematic diagram of the MAM grid electrode and an optical microscope (OM) image. The calculated dependence of total sheet resistance and optical transmittance of MAM grid electrodes and Ag grid electrodes with different Ag thicknesses is shown in Fig. 2b. All these values were calculated at the same FF of 0.24.

From this data, we can assume that the optical transmittance of MAM grid electrodes is reduced from 95 to 77% with increasing Ag grid thickness from 20 to 75 nm, compared with Ag grid electrodes from 88 to 76% for the same Ag grid thickness range. The calculated dependence of total sheet resistance is also decreased as increasing the Ag grid thickness in the range from 10.33 (20 nm) to 1.45 (75 nm) as shown in Fig. 2b. The optical transmittance and the sheet resistance of MAM grid electrodes and Ag (x nm) grid electrodes with an FF of 0.24 are shown in Fig. 2c. These figures indicate that the experiment results are in good agreement with the calculated results, as shown in Fig. 2b, c. With a decreased Ag layer thickness, the MAM grid electrodes' optical transmittance dramatically increased over that of the Ag grid electrodes even though the MAM grid electrodes' sheet resistance lightly increased compared to the Ag grid electrodes. To optimize the thickness of Ag, we calculated the Haack figure of merit (Φ_H) value as defined by following equation [27]:

$$\Phi_H = \frac{T^{10}}{R_s}$$

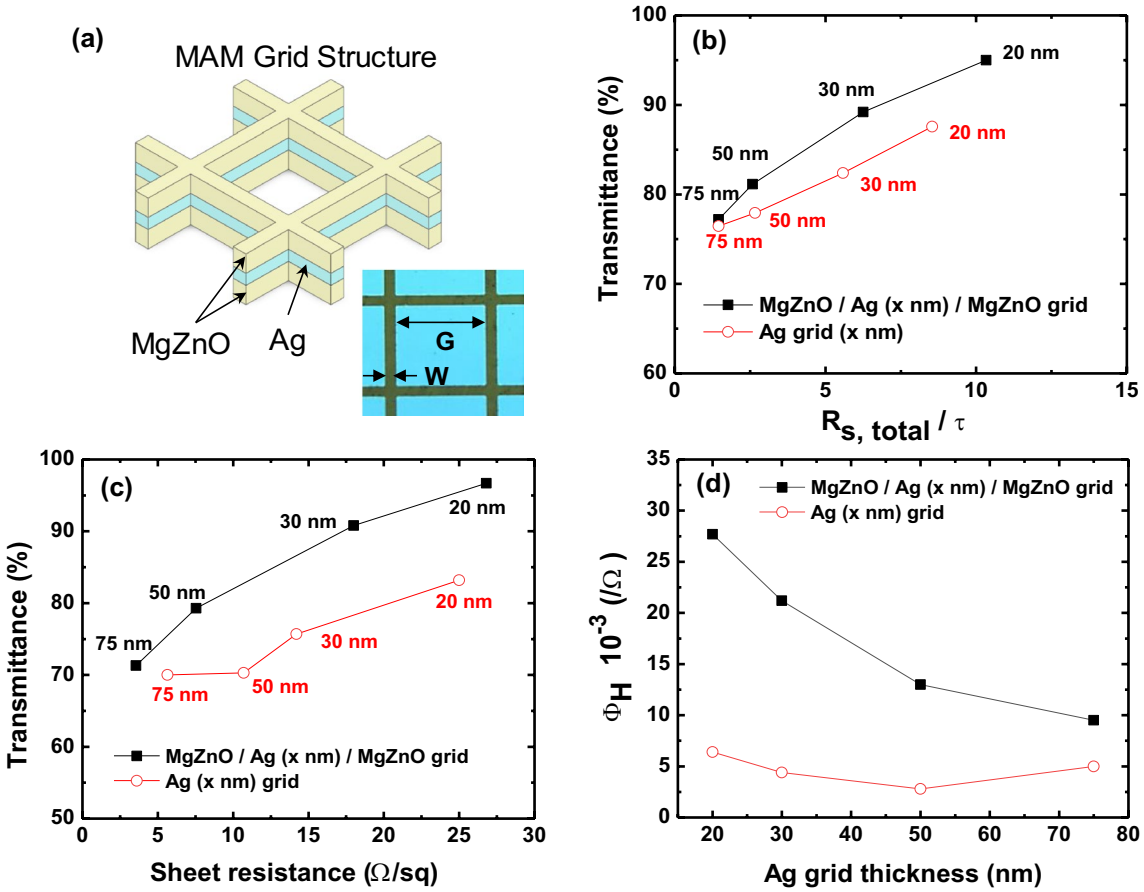

Fig. 2 **a** Schematic and OM image of MAM grid electrode and **b** calculated optical transmittance at 550 nm and $R_{s,\ total}/\tau$. **c** Experimental optical transmittance at 550 nm and sheet resistance of MAM grid electrodes and Ag grid electrodes for various Ag layer thicknesses, and **d** Haack Φ_H value of grid electrodes

where R_s is the sheet resistance and T is the optical transmittance at a 550 nm wavelength. The maximum Φ_H of $26.7 \times 10^{-3}/\Omega$ can be obtained for MAM grid electrodes when their Ag layer is 20 nm-thick and their FF is 0.24 as shown in Fig. 2d.

To characterize transmittance dependence on FF, we explored the results for the FF of MAM grid electrodes and Ag grid electrodes having a 20 nm-thick Ag layer as shown in Fig. 3a. The optical transmittance of MAM grid electrodes in a broad wavelength region (400 ~ 1100 nm) is higher than that of Ag grid electrodes regardless of FF as shown in Fig. 3b. These results show that transmittance decrease with increasing FF was lower for MAM grid electrodes than for Ag grid electrodes because Ag grid lines reflect more light than MAM grid lines. However, the transmittance of MAM grid electrodes at the 550 nm wavelength is relatively independent of FF as opposed to the longer wavelength regions (> 550 nm) where FF has a dramatic effect on transmittance because of reflectance by free electrons. Table 1 summarizes the values of R_s, T (transmittance at 550 nm), T_{av} (average transmittance in the wavelength range from 400 to 1100 nm) and Φ_H of the MAM grid electrodes and Ag grid electrodes as a function of the FF. The highest Φ_H value for the MAM grid electrode is 8.1 and this value is approximately three-fold higher than that of the Ag grid electrode for the same Ag thickness.

It is well known that the Ag layer is easily oxidized and disintegrated when exposed to high humidity and high-temperature environments [9, 12].

To investigate the thermal and chemical stability of MAM and Ag grid electrodes, they were annealed for 1 h at various temperatures and were exposed to UV-ozone for various exposure times.

Figure 4a shows the sheet resistance change (R_s/R_0, where R_s is the sheet resistance after annealing process and R_0 is the initial sheet resistance before annealing) of MAM and Ag grid electrodes as a function of annealing temperature.

Compared to as-deposited Ag grid and MAM grid electrodes as shown in Fig. 4g, h, we could not measure the sheet resistance of Ag grid electrode because the Ag grid lines were transformed into Ag nanoparticles after annealing

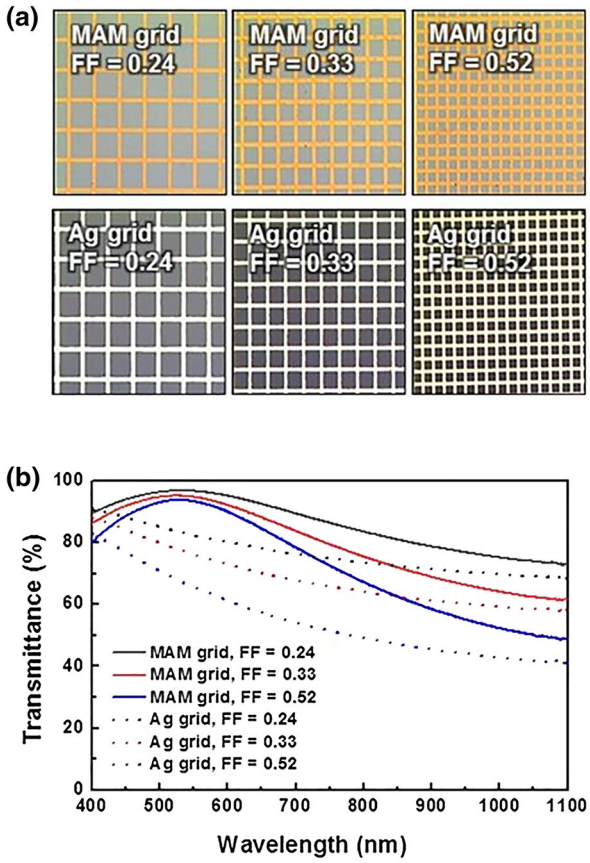

Fig. 3 **a** OM images and **b** optical transmittance of MAM grid electrodes and Ag grid electrodes for various FFs

of 250 °C, as shown in Fig. 4b. However, the sheet resistance of MAM grid electrodes continuously decreased until the annealing temperature of 350 °C. Previous studies have reported that the sheet resistance of oxide/metal/oxide film was decreased by annealing process because crystal quality of oxide layers was improved [29, 30]. The enhancement of MgZnO crystallinity decreases the sheet resistance of MAM grid electrode and inhibits migration of Ag atoms and Ag oxidation as shown in Fig. 4c. However, the sheet resistance of MAM grid electrodes increased above 350 °C because Ag atoms diffuse into MgZnO layer [28].

Figure 4d shows the sheet resistance changes of MAM and Ag grid electrodes with various exposure times to UV-ozone in a study of chemical stability. The sheet resistance of the Ag grid electrodes dramatically increased with longer UV-ozone exposure times due to corrosion of the Ag grid layer as shown in Fig. 4e [30]. In contrast, the sheet resistance of MAM grid electrodes after exposure to UV-ozone for 18 min showed similarity to its initial value as shown in Fig. 4d. Moreover, even the surface morphology of MAM grid lines was not changed as shown in Fig. 4f. These results indicate that MAM grid electrodes have superior resistance to oxidation than Ag grid electrodes because of their protective MgZnO layers.

4 Conclusion

In conclusion, we investigated highly durable MAM grid electrodes with high electrical and optical performance. A MAM grid electrode with a 20 nm-thick Ag layer and an FF of 0.24 shows a high average transmittance of 85.8% over the broad wavelength region of 400–1100 nm and a low sheet resistance of 26.9Ω/sq. The Φ_H of the MAM grid electrode is approximately threefold higher than that of an Ag grid electrode for the same Ag thickness. Furthermore, MAM grid electrodes have higher harsh environment stability than Ag grid electrodes. These results indicate that MAM grid electrodes can be a viable alternative to metal-based grid electrodes in solar cells, touch-screen panels, and flexible organic applications.

Table 1 Sheet resistance, optical transmittance at 550 nm, average transmittance from 400 to 1100 nm, and Φ_H values of MAM grid electrodes and Ag grid electrodes for various FF

	FF	R_s (Ω/sq)	T (%) (550 nm)	T_{av} (%) (400 ~ 1100 nm)	$\Phi_H \times 10^{-3}$ (Ω^{-1}) (400 ~ 1100 nm)
MAM grid	0.24	26.8	96.7	85.8	8.1
	0.33	21.9	94.7	79.1	4.4
	0.52	13.2	93.3	72.2	2.9
Ag grid	0.24	25	83.2	76.5	2.75
	0.33	20.2	76.1	68.3	1.09
	0.52	11.5	65.6	55.0	0.22

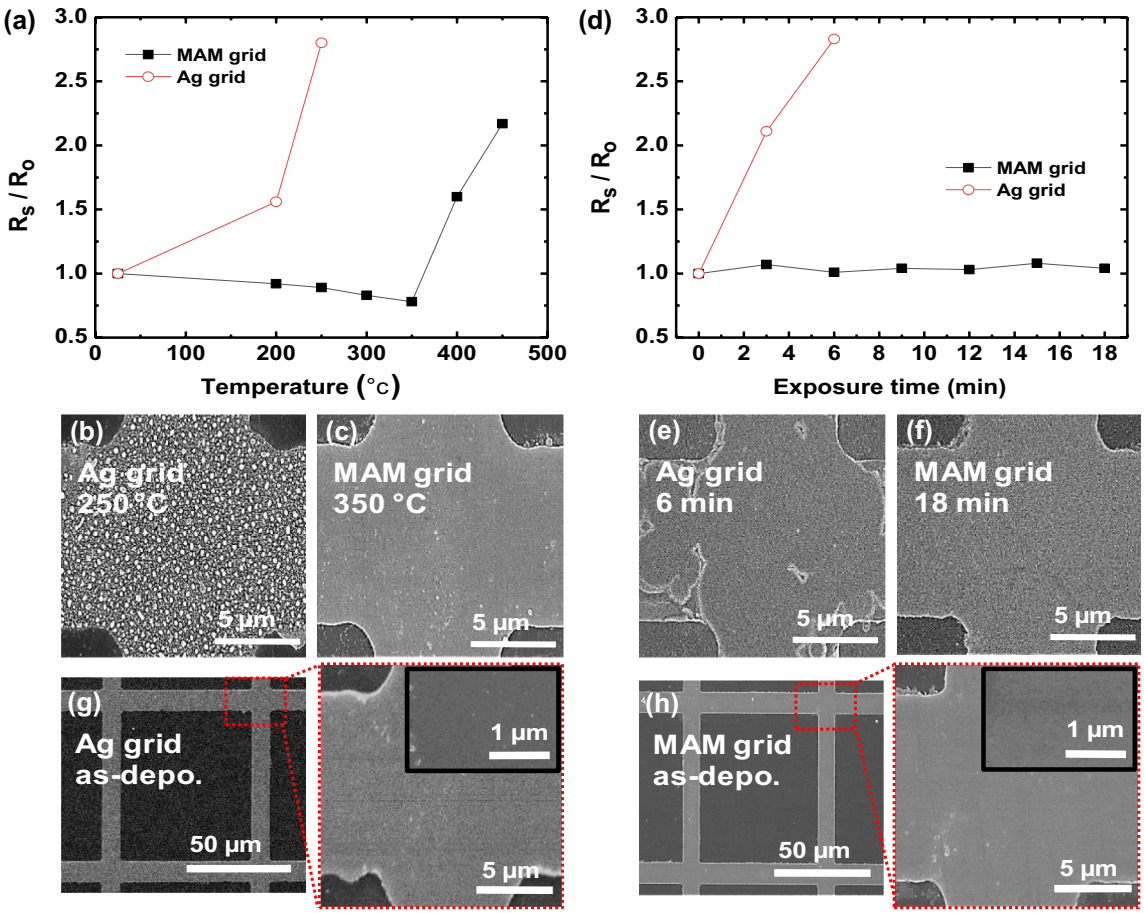

Fig. 4 **a** Resistance change of MAM grid electrodes and Ag grid electrodes for various annealing temperatures. SEM images of **b** Ag grid and **c** MAM grid electrodes after annealing processes. **d** Resistance change of them electrodes for various UV-ozone exposure times. SEM images of **e** Ag grid and **f** MAM grid after exposure to UV-ozone treatment and as-deposited **g** Ag grid and **h** MAM grid electrodes (red-dashed and inset: high magnification images)

Acknowledgements This research was supported by the MSIT (Ministry of Science and ICT), Korea, under the ITRC (Information Technology Research Center) support program (IITP-2019-2018-0-01426) supervised by the IITP(Institute for Information & Communications Technology Planning & Evaluation), and by Human Resources Program in the Transportation Specialized Lighting Core Technology Development (No. N0001364) and by the Technology Innovation Program (20002694, Gas sensor) Granted financial resource from the Ministry of Trade, Industry & Energy, Republic of Korea.

Compliance with Ethical Standards

Conflict of interest On behalf of all authors, the corresponding author states that there is no conflict of interest.

References

1. Morales-Masis, M., De Wolf, S., Woods-Robinson, R., Ager, J. W., & Ballif, C. (2017). Transparent electrodes for efficient optoelectronics. *Advanced Electronic Materials, 3*(1600529), 1–17.
2. Ellmer, K. (2012). Past achievements and future challenges in the development of optically transparent electrodes. *Nature Photonics, 6*(809), 809–817.
3. Lee, S. H., Kim, S. W., Park, C. W., Jeong, H. E., Ok, J. G., & Kwak, M. K. (2017). Scalable fabrication of flexible transparent heaters comprising continuously created metallic micromesh patterns incorporated with biomimetic anti-reflection layers. *International Journal of Precision Engineering and Manufacturing-Green Technology, 4*(2), 177–181.
4. Ye, S., Rathmell, A. R., Chen, Z., Stewart, I. E., & Wiley, B. J. (2014). Metal nanowire networks: The next generation of transparent conductors. *Advanced Materials, 26,* 6670–6687.
5. Lee, H. J., Oh, S., Cho, K. Y., Jeong, W. L., Lee, D. S., & Park, S. J. (2018). Spontaneous and selective nanowelding of silver nanowires by electrochemical ostwald ripening and high electrostatic potential at the junctions for high-performance stretchable transparent. *ACS Applied Materials and Interfaces, 10,* 14124–14131.
6. Park, J., & Hwang, J. (2014). Fabrication of a flexible Ag-grid transparent electrode using ac based electrohydrodynamic jet printing. *Journal of Physics. D. Applied Physics, 47*(405102), 1–7.

7. Park, J. H., Lee, D. Y., Kim, Y. H., Kim, J. K., Lee, J. H., Park, J. H., et al. (2014). Flexible and transparent metallic grid electrodes prepared by evaporative assembly. *ACS Applied Materials and Interfaces, 6,* 12380–12387.
8. Jang, Y., Kim, J., & Byun, D. (2013). Invisible metal-grid transparent electrode prepared by electrohydrodynamic (EDH) jet printing. *Journal of Physics D. Applied Physics, 46*(155103), 1–5.
9. Hong, S., Yeo, J., Kim, G., Kim, D., Lee, H., Kwon, J., et al. (2013). Nonvacuum, maskless fabrication of a flexible metal grid transparent conductor by low-temperature selective laser sintering of nanoparticle ink. *ACS Nano, 7*(6), 5024–5031.
10. Li, T. C., & Chang, R. C. (2014). Improving the performance of ITO thin films by coating PEDOT:PSS. *International Journal of Precision Engineering and Manufacturing-Green Technology, 1*(4), 3329–3334.
11. Son, J. M., Lee, C., Hong, S. K., Kang, J. J., & Cho, Y. H. (2017). Fast thermal response of silicon nanowire-heater for heat shock generation. *International Journal of Precision Engineering and Manufacturing-Green Technology, 4*(1), 42–45.
12. Rathmell, A. R., Nguyen, M., Chi, M., & Wiley, B. J. (2012). Synthesis of oxidation-resist cupronickel nanowires for transparent conducting nanowire networks. *Nano Letters, 12,* 3193–3199.
13. Im, H. G., Jin, J., Ko, J. H., Lee, J., Lee, J. Y., & Bae, B. S. (2014). Flexible transparent conducting composite films using a monolithically embedded AgNW electrode with robust performance stability. *Nanoscale, 6,* 711–715.
14. Sharma, V., Kumar, P., Kumar, A., Surbhi, A. K., & Sachdev, K. (2017). High-performance radiation stable ZnO/Ag/ZnO multilayer transparent conductive electrode. *Solar Energy Materials and Solar Cells, 169,* 122–131.
15. Maniyara, R. A., Mkhitaryan, V. K., Chen, T. L., Ghosh, D. S., & Pruneri, V. (2016). An antireflection transparent conductor with ultralow optical loss (< 2%) and electrical resistance (< 6 Ωsq^{-1}). *Nature Communications, 7*(13771), 1–8.
16. Ren, N., Zhu, J., & Ban, S. (2017). Highly transparent conductive ITO/Ag/ITO trilayer films deposited by RF sputtering at room temperature. *AIP Advances, 7,* 1–7.
17. Wang, C. T., Ting, C. C., Kao, P. C., Li, S. R., & Chu, S. Y. (2016). Improvement of optical and electrical characteristics of MoO_3/Ag film/MoO_3 flexible transparent electrode with metallic grid. *Journal of Applied Physics, 120,* 1–7.
18. Lee, H. J., Kang, J. W., Hong, S. H., Song, S. H., & Park, S. J. (2016). $Mg_xZn_{1-x}O$/Ag/$Mg_xZn_{1-x}O$ multilayers as high-performance. *ACS Applied Materials & Interfaces, 8,* 1565–1570.
19. Guillén, C., & Herrero, J. (2011). TCO/meta/TCO structures for energy and flexible electronics. *Thin Solid Films, 520,* 1–17.
20. Kim, H. J., Lee, S. H., Lee, J., Lee, E. S., Choi, J. H., Jung, J. H., et al. (2014). High-durable AgNi nanomesh film for a transparent conducting electrode. *Small (Weinheim an der Bergstrasse, Germany), 10*(18), 3767–3774.
21. Kim, D. J., Kim, H. J., Seo, K. W., Kim, K. H., Kim, T. W., & Kim, H. K. (2015). Indium-free, highly transparent, flexible Cu_2O/Cu/Cu_2O mesh electrodes for flexible touch screen panels. *Scientific Reports, 5*(16838), 1–10.
22. Han, H., Theodore, N. D., & Alford, T. L. (2008). Improved conductivity and mechanism of carrier transport in zin oxide with embedded silver layer. *Journal of Applied Physics, 103,* 1–8.
23. Zhang, D., Wang, P., Murakami, R., & Song, X. (2010). Effect of an interface charge density wave on surface plasmon in ZnO/Ag/ZnO thin films. *Applied Physics Letters, 96,* 1–3.
24. Chin, H. A., Cheng, I. C., Huang, C. I., Wu, Y. R., Lu, W. S., Lee, W. L., et al. (2010). Two dimensional electron gases in polycrystalline MgZnO/ZnO heterostructures grown by rf-sputtering process. *Journal of Applied Physics, 108,* 1–4.
25. Chi, C. T., Cheng, I. C., & Chen, J. Z. (2012). Bandgap tuning of MgZnO in flexible transparent n + -ZnO:al/n-MgZnO/p-CuAlOx: Ca diodes on polyethylene terephthalate substrates. *Journal of Alloys and Compounds, 544,* 111–114.
26. Ghosh, D. S., Chen, T. L., & Pruneri, V. (2010). High figure-or-merit ultrathin metal transparent electrodes incorporating a conductive grid. *Applied Physics Letters, 96,* 1–3.
27. Haacke, G. (1976). New figure of merit for transparent conductors. *Journal of Applied Physics, 47*(9), 4086–4089.
28. Liu, W. S., Liu, Y. H., Chen, W. K., & Hsueh, K. P. (2013). Transparent Conductive Ga-doped MgZnO/Ag/Ga-doped MgZnO sandwich structure with improved conductivity and transmittance. *Journal of Alloys and Compounds, 564,* 105–113.
29. Sahu, D. R., Lin, S. Y., & Huang, J. L. (2008). Investigation of conductive and transparent Al-doped ZnO/Ag/Al-doped ZnO multilayer coatings by electron beam evaporation. *Thin Solid Films, 516,* 4728–4732.
30. Chen, Z. Y., Liang, D., Ma, G., Frankel, G. S., Allen, H. C., & Kelly, R. G. (2013). Influence of UV irradiation and ozone on atmospheric corrosion of bare silver. *Corrosion Engineering, Science and Technology, 45*(2), 169–180.

Hyo-ju Lee received the Ph.D. (2018) in Materials Science and Engineering in Gwangju Institute of Science and Technology, Korea, from 2013 to 2018. He is a staff engineer in Samsung Electro-mechanics since 2018. His recent research is focused on the development of low profile multi layer ceramic capacitor (MLCC).

Ki-Yeop Cho received his M.S. degree (2018) from School of Materials Science and Engineering at Gwangju Institute of Science and Technology, Korea, and he is currently a Ph.D. candidate. His research interests presently include the design of lithium metal anode, design of novel energy storage systems and electrochemical techniques for material modification.

Semi Oh received the Ph.D. degree (2018) in Materials Science and Engineering in Gwangju Institute of Science and Technology, Korea, from 2013 to 2018. She is a Postdoctoral researcher in Electrical Engineering and Computer Science in University of Michigan since 2018. Her recent research interest is focused on the semiconductor and dielectric nanostructure synthesis and device applications such as light emitters, gas sensors, and photoelectrochemical devices.

So-Yeon Park received the M.S. degree (2020) in the Department of Advanced Convergence Technology in Korea Polytechnic University (KPU) and she is currently a Ph.D student under supervision of Prof. Kyoung-Kook Kim. Her research is focused on the finger printer using dielectric and semiconductor nanostructures.

Ye-Bin Im received the B.S. degree (2019) in the Department of Nano Optical Engineering in Korea Polytechnic University (KPU). She is currently a M.S. student under supervision of Prof. Kyoung-Kook Kim at the Department of Advanced Convergence Technology, KPU. Her research is focused on the finger printer using dielectric and semiconductor nanostructures.

Suyeon Son received the B.S. degree (2019) in the Department of Nano Optical Engineering in Korea Polytechnic University (KPU). He is currently a M.S. student under supervision of Prof. Kyoung-Kook Kim at the Department of Advanced Convergence Technology, KPU. His research is focused on the flexible display and thin film transistor using oxide-based transparent conducting layers.

Yong-Jin Yoon received the Ph.D. degree in mechanical engineering from Stanford University, in 2009. Dr. Yoon is currently an Associate Professor, Department of Mechanical Engineering, KAIST. His research interest lies in applied mechanics, vibration, 3-D printing, and bio-acoustics. With a Ph.D. background on mathematical modeling of hearing mechanics, he spent years in Stanford working on computational mechanics and theoretical modeling. His current research activities include developing resonator type MEMS sensors, lab-on-a-chip devices, hearing micromechanics, and cell/tissue engineering with 3-D printing technology.

Seong-Ju Park is a Distinguished Professor in School of Materials Science and Engineering in Gwangju Institute of Science and Technology in Korea. He received the Ph.D. from Cornell University in 1985, and worked as Postdoctoral fellow at IBM T.J. Watson Research Center, USA, from 1985 to 1987. He was a Professor in School of Materials Science and Engineering in Gwangju Institute of Science and Technology in Korea from 1995 to 2018. His research interests focus on the nitride and zinc oxide based light-emitting diode and optoelectronic devices, as well as the multifunctional nano-sensing devices, transparent conducting electrodes for the various applications in display and energy.

Kyoung-Kook Kim received the Ph.D. degree in Materials Science and Engineering in GIST, in 2003. Prof. Kim worked as Postdoctoral fellow at Nanodevice Research Group of Nanomaterials Laboratory in National Institute for Materials Science (NIMS), and Research Center for Photovoltaics in National Institute of Advanced Industrial Science and Technology (AIST), Tsukuba in Japan, and Project Leader for Development of vertical LED and Nano-LED, R&D Staff Member of Photonics Team in Samsung Advanced Institute Technology (SAIT). Prof. Kim is currently an Professor, Department of Nano & Semiconductor Engineering, Director of Research Institute of Advanced Convergence Technology, Korea Polytechnic University (KPU), Korea. His current research interests are Nanostructure synthesis using oxide and nitride materials, Flexible materials by convergence technology with oxide and metal, and Photonic and electronic devices for multifunctional sensors and power devices.